Int. J. Electron. Commun. (AEÜ) 87 (2018) 158–163

Contents lists available at ScienceDirect

Int. J. Electron. Commun. (AEÜ)

journal homepage: www.elsevier.com/locate/aeue

Regular paper

Compact low-loss microstrip diplexer using novel engraved semi-patch cells for GSM and WLAN applications

Abbas Rezaei[a,*], Leila Noori[b]

[a] Department of Electrical Engineering, Kermanshah University of Technology, Kermanshah, Iran
[b] Young Researchers and Elite Club, Kermanshah Branch, Islamic Azad University, Kermanshah, Iran

ARTICLE INFO

Keywords:
Diplexer
Microstrip
Compact
Harmonics
Insertion loss

ABSTRACT

This paper presents a novel microstrip diplexer constructed by integrating the engraved semi-patch cells. It operates at 1.8 GHz for global system for mobile communication (GSM) and 2.4 GHz for wireless local area network (WLAN). The introduced structure is well miniaturized so that it has a compact size of 0.022 λg^2. The others advantages of the proposed diplexer are the low insertion losses less than 0.16 dB, good in-band channel isolation higher than 34 dB and two wide fractional bandwidths. Moreover, 1st, 2nd and 3rd harmonics are attenuated with the maximum level of −20 dB. A harmonic attenuation method is presented based on analyzing the resonance modes. In order to verify the simulation results, the designed diplexer is fabricated and measured. The simulation and measurement results are in a good agreement.

1. Introduction

Planar microstrip diplexers with high performance are widely demanded by the modern radio receivers or transmitters on different frequency bands where a multiband antenna is used on a tower with a common feedline. In order to separate frequencies of a multiband/wideband antenna, two ports are multiplexed onto a common port. Generally, a well-designed diplexer has the features of compact size, high isolation, low losses, high selectivity and low harmonic levels. Recently, various types of microstrip diplexers have been reported [1–10]. To design these microstrip diplexers, folded open loop ring structures in [1], triangular open loop resonators in [2], step impedance resonators loaded by interdigital capacitors in [3], steps and coupled lines in [4] and coupled dual-mode stub-loaded resonators in [5] have been utilized. In [6], coupled lines and spiral cells, in [7] electrically-coupling half-wavelength resonators, in [8] the loops consisting of coupled lines, step impedances and low impedance sections, in [9] spiral rings connected to interdigital capacitors and in [10] coupled rings loaded by T-shape cells have been used. However, the common disadvantage of these reported diplexers is their large size. The presented diplexers in [1,5,7] and [9] have large insertion losses while the return losses in [2,4] and [8] are high. Despite having a high isolation which is an important issue, the designed diplexers in [1,3,4,6], and [8,9] could not get it. A new challenge in a diplexer design is harmonic suppression. Nevertheless, only in [1] and [2] harmonic attenuations have been well done while the others [3–10] could not attenuate the 3rd harmonics.

This work presents a compact high performance microstrip diplexer based on a novel geometrical structure consisting of the engraved semi-patch cells. It is designed to solve the problems of the previous works in terms of improving insertion loss, obtaining high isolation and high selectivity and also miniaturizing. Moreover, a relatively good return loss is achieved. Meanwhile, the bandwidths are relatively wide and flat enough. The introduced diplexer operates at 1.8 GHz for GSM and 2.4 GHz for IEEE 802.11 WLAN applications. The designing method is based on proposing a LC circuit of the resonator, analyzing the even and odd modes and finally finding a method to tune the resonance frequency and attenuate the harmonics.

2. Design and theory

Fig. 1(a), depicts our basic structure. It consists of a semi-patch cell connected to the feedlines. The transition of the input port can be descripted based on the LC model of basic structure. Because to create a passband we need a passive LC circuit. A capacitor can be provided by a patch cell while an inductor will be created by the other thinner parts. The reason of choosing a patch capacitor is to save the size. The thinner cells can provide many inductors so that a high degree of freedom to control the performance is obtained by utilizing the engraved semi-patch structure. Therefore, to have a large number of inductors and miniaturization simultaneously, some parts of the basic structure are engraved. An approximated LC model of the introduced structure is shown in Fig. 1(b). In the LC circuit, the inductances of stubs with the

* Corresponding author.
E-mail addresses: a.rezaee@kut.ac.ir (A. Rezaei), Leila_noori62@yahoo.com (L. Noori).

https://doi.org/10.1016/j.aeue.2018.02.022
Received 22 October 2017; Accepted 21 February 2018
1434-8411/

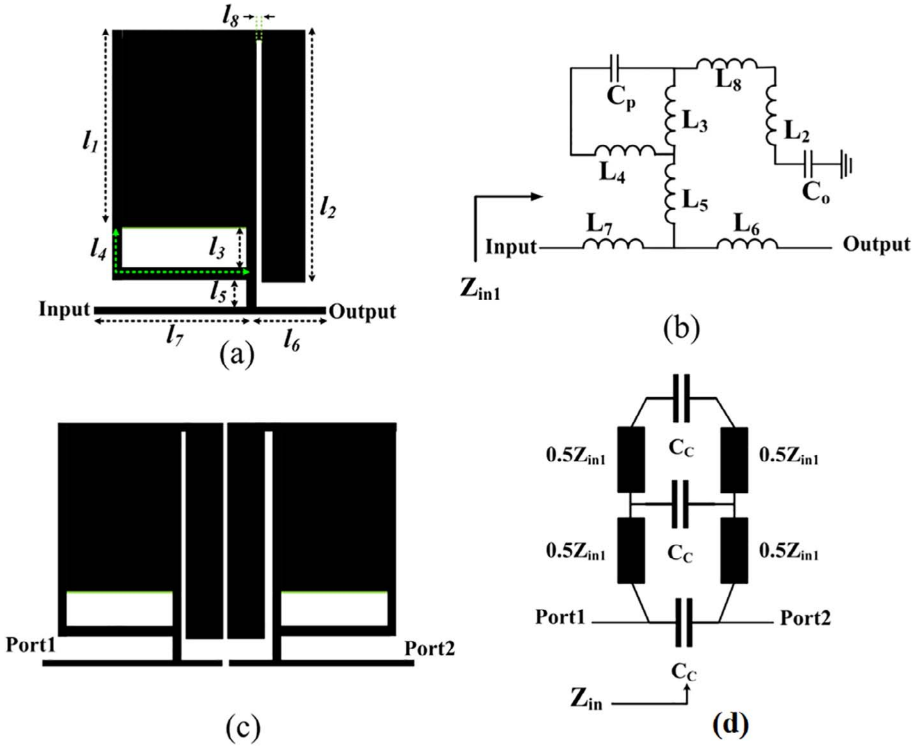

Fig. 1. (a) Proposed basic structure, (b) the LC model of proposed basic structure, (c) the proposed resonator and (d) the equivalent circuit of proposed resonator.

physical lengths l_2, l_3, l_4, l_5, l_6, l_7 and l_8 are L_2, L_3, L_4, L_5, L_6, L_7 and L_8 respectively. Cp is the patch capacitor and Co is the open end capacitor. In this LC circuit, the effects of bents and steps are ignored because they have only a significant role at the frequencies higher than 10 GHz. The proposed resonator and its equivalent circuit are presented in Fig. 1(c) and 1(d), respectively. The proposed resonator consists of two similar basic structures, which are coupled to each other. In Fig. 1(d), the capacitors of coupling are presented by Cc. The equivalent circuit of coupling is an approximated model [11]. In the exact model, the number of coupling capacitors will be increased.

The equivalent impedance of the basic structure viewed from the input port when the output port is opened, is calculated as follows:

$$Z_{in1} = \frac{(j\omega L_4 + \frac{1}{j\omega C_P}) \times j\omega L_3}{j\omega L_4 + \frac{1}{j\omega C_P} + j\omega L_3} + j\omega L_a + \frac{1}{j\omega C_o}$$
$$= j\frac{1 + \omega^3 C_O C_P[L_4L_3 + L_aL_4 + L_aL_3] + \omega^2 C_P(L_4 + L_3) - \omega C_O[L_3 + C_P L_a]}{C_O - \omega^2(L_4 + L_3)C_P C_O} for$$
$$: L_a = L_2 + L_8 + L_5 + L_7 \tag{1}$$

In Eq. (1), ω is an angular frequency. From the equivalent circuit of introduced resonator, the input impedance between ports 1 and 2 can be written as follows:

$$Z_{in} = \frac{\left[\frac{(Z_{in1} + \frac{1}{j\omega Cc})\frac{1}{j\omega Cc}}{Z_{in1} + \frac{2}{j\omega Cc}} + Z_{in1}\right]\frac{1}{j\omega Cc}}{\frac{\left(Z_{in1} + \frac{1}{j\omega Cc}\right)\frac{1}{j\omega Cc}}{Z_{in1} + \frac{2}{j\omega Cc}} + Z_{in1} + \frac{1}{j\omega Cc}}$$
$$= \frac{1 + j\omega CcZ_{in1}(Z_{in1} j\omega Cc + 3)}{j\omega Cc[j\omega CcZ_{in1}(4 + Z_{in1} j\omega Cc) + 3]} \tag{2}$$

2.1. Even and odd modes analysis

Due to having a symmetrical structure, we can analyze the even and odd modes for the proposed resonator. In order to create the resonance frequencies, Z_{in} (for the odd mode) and Z_{in}^{-1} (for the even mode) must be zero. Accordingly, the even and odd mode resonance conditions can be extracted from Eq. (2) as follow:

$$Odd\,Mode: 1 + j\omega_o CcZ_{in1}(Z_{in1} j\omega_o Cc + 3)$$
$$= 0 \Rightarrow \omega_o^2(Cc^2 Z_{in1}^2) - \omega_o(j3CcZ_{in1}) - 1 = 0 \Rightarrow \omega_o = j\frac{(3 \pm \sqrt{5})}{2CcZ_{in1}}$$
$$Even\,Mode: j\omega_e Cc[j\omega_e CcZ_{in1}(4 + Z_{in1} j\omega_e Cc) + 3]$$
$$= 0 \Rightarrow \omega_e^2(Cc^2 Z_{in1}^2) - \omega_e(j4CcZ_{in1}) - 3 = 0 \Rightarrow \omega_e = j\frac{(4 \pm 2)}{2CcZ_{in1}} \tag{3}$$

where ω_o and ω_e are the odd and even modes angular resonance frequencies. From Eq. (1), Z_{in1} depends on ω, therefore by substituting Eq. (1) into Eq. (3) we can obtain the following results for the odd mode:

$$Odd\,Mode: \begin{cases} Z_{in1} = j\frac{1 + \omega_o^3 C_O C_P[L_4L_3 + L_aL_4 + L_aL_3] + \omega_o^2 C_P(L_4 + L_3) - \omega_o C_O[L_3 + C_P L_a]}{C_O - \omega_o^2(L_4 + L_3)C_P C_O} \\ 1 + j\omega_o CcZ_{in1}(Z_{in1} j\omega Cc + 3) = 0 \Rightarrow \frac{-1}{j\omega_o CcZ_{in1}} = Z_{in1} j\omega_o Cc + 3 \end{cases} \Rightarrow$$
$$\frac{C_O - \omega_o^2(L_4 + L_3)C_P C_O}{\omega_o Cc + \omega_o^4 CcC_O C_P[L_4L_3 + L_aL_4 + L_aL_3] + \omega_o^3 CcC_P(L_4 + L_3) - \omega_o^2 CcC_O[L_3 + C_P L_a]}$$
$$= -\frac{\omega_o Cc + \omega_o^4 CcC_O C_P[L_4L_3 + L_aL_4 + L_aL_3] + \omega_o^3 CcC_P(L_4 + L_3) - \omega_o^2 CcC_O[L_3 + C_P L_a]}{C_O - \omega_o^2(L_4 + L_3)C_P C_O} + 3 \Rightarrow$$
$$\frac{C_O - \omega_o^2 bC_O}{\omega_o Cc + \omega_o^4 Cca + \omega_o^3 Ccb - \omega_o^2 cCc} = -\frac{\omega_o Cc + \omega_o^4 Cca + \omega_o^3 Ccb - \omega_o^2 cCc}{C_O - \omega_o^2 bC_O} + 3\, for$$
$$: \begin{cases} a = C_O C_P[L_4L_3 + L_aL_4 + L_aL_3] \\ b = C_P(L_4 + L_3) \\ c = C_O[L_3 + C_P L_a] \end{cases} \Rightarrow$$
$$\frac{C_O - \omega_o^2 bC_O}{\omega_o Cc + \omega_o^4 Cca + \omega_o^3 Ccb - \omega_o^2 cCc} + \frac{\omega_o Cc + \omega_o^4 Cca + \omega_o^3 Ccb - \omega_o^2 cCc}{C_O - \omega_o^2 bC_O} + 3 = 0 \Rightarrow$$
$$\omega_o^4 a + \omega_o^3 b - \omega_o^2(c - 0.5b(3 \pm \sqrt{5})C_O Cc^{-1}) + \omega_o - 0.5(3 \pm \sqrt{5})C_O Cc^{-1} = 0 \tag{4.a}$$

Similarly, the following results are obtained for the even mode: